

## Impact of massive material injection on runaway electron generation

O. Linder<sup>1</sup>, E. Fable<sup>1</sup>, F. Jenko<sup>1</sup>, G. Papp<sup>1</sup> and G. Pautasso<sup>1</sup>

<sup>1</sup> *Max-Planck-Institut für Plasmaphysik, 85748 Garching, Germany*

**1. Introduction** In current carrying fusion devices, the sudden loss of thermal energy, referred to as disruptions, poses a serious threat to the integrity of the plasma vessel, as relativistic runaway electrons (REs) generated in the process may cause intense localised damage to plasma facing components. In future high- $I_p$  devices such as ITER, the risk of replacing a large fraction of the pre-disruptive current by REs is significantly greater than in present-day devices due to exponentiation of a post-disruption RE seed. As countermeasure, massive material injection (MMI) is foreseen in ITER. Yet in dedicated experiments of present-day devices such as ASDEX Upgrade (AUG), clear correlations between the amount of injected material, the plasma response and the RE behaviour are challenging to observe [1–3]. In this work, the software-kit ASTRA-STRABL is presented as a complementary method for the study of MMI scenarios and the impact of (simple) injection schemes on RE generation is discussed.

**2. Model description** The interaction between background plasma, injected material and REs is to be studied by transport modelling of particles and heat with the 1.5D transport code ASTRA [4] coupled to the impurity radiation code STRABL [5]. This toolset was previously used i.a. to study the pre-thermal quench of AUG massive gas injection (MGI) experiments [6], but is enhanced for the purposes of this study. Evolution of the background plasma and the magnetic equilibrium is performed by ASTRA through  $\partial_t f = V'^{-1} \partial_\rho \{ V' g [ D \partial_\rho f - v f ] \} + \sum_j S_j$ , where  $f$  is any of the evolved quantities ( $n_e$ ,  $T_e$ ,  $T_i$ ,  $\Psi$ ). Impurity radiation provided by STRABL is treated as electron energy sink  $S_{\text{rad}}$ . Impurity electrons are considered in the evolution of  $n_e$ . STRABL in turn solves transport equations of the above type for each individual impurity ionisation stage using ASTRA-provided plasma and geometric profiles. The transport coefficients  $D$  and  $v$  are calculated by NEOART (neoclassical transport) or may be provided externally (anomalous transport). Atomic processes are described through tabulated rate coefficients (ADAS) and prescribed as sources/sinks  $S$ , thus allowing simulation of non-equilibrium phenomena. To simulate MGI, multiple neutral impurity populations are employed for the treatment of external and recombined neutrals with different distribution functions  $f(\rho, \mathbf{v}, t)$ . The former neutrals are assumed to propagate into the plasma core with thermal velocity.

REs are treated in ASTRA as a separate species, whose generation is described by the fluid equations  $S_D = c e k_D n_e v_e (E_D/E_{\parallel})^h \exp \left( -\lambda E_D/E_{\parallel} - \gamma \sqrt{E_D/E_{\parallel}} \right)^1$  for small-angle momentum

<sup>1</sup> $E_{\parallel}$  is the parallel,  $E_D$  the Dreicer and  $E_c$  the critical electric field. See [7, 8] for factors  $E_D$ ,  $E_c$ ,  $k_D$ ,  $k_{av}$ ,  $h$ ,  $\lambda$ ,  $\gamma$ .

space diffusion (Dreicer mechanism) [7] and  $S_{av} = ce k_{av} n_{RE} v_e (E_{\parallel}/E_c - 1) / \ln \Lambda$  for large-angle knock-on collision (avalanche mechanism) [8]. The non-negligible impact of partially ionised impurities on the critical electric field  $E_c$  [9] and on the avalanche growth rate  $S_{av}$  [10] is to be taken into account in future work. The RE current is added to the existing plasma current, thus affecting  $\Psi$ -evolution in ASTRA.

**3. RE model verification** The RE fluid model in ASTRA is validated by comparing the calculated RE current generated in an artificial disruption against calculations by the disruption code GO [11]. For this purpose, simulation parameters resembling AUG #33108 [2, 3] are chosen ( $I_0 = 752$  kA and  $Z_{eff} = 1$ ). In this discharge, argon is injected at

$t_{MGI} = 1$  s into a low-density (line averaged  $n_e = 2.8 \times 10^{19} \text{ m}^{-3}$ ), circular limiter plasma with peaked temperature profile (2.6 MW of central ECRH pre-injection) to induce a disruption. Electron density and temperature measurements are averaged over the last 50 ms prior to injection (see Fig. 1) and used as initial profiles in ASTRA. In the simulations, the electron temperature is quenched exponentially as  $T_e(\rho, t) = T_e(\rho, 0)[(1 - T_{e,f}/T_e(0, 0)) \exp(-t/\tau) + T_{e,f}/T_e(0, 0)]$  on a time scale  $\tau$  down to  $T_{e,f}$  (preserving the shape of the initial temperature profile). The thermal quench time and final central electron temperature are varied across multiple simulations between  $0.1 \text{ ms} \leq \tau \leq 10.0 \text{ ms}$  and  $1 \text{ eV} \leq T_{e,f} \leq 100 \text{ eV}$ , thus covering – but also extending – the AUG-relevant parameter space ( $t_0 \leq 1.0 \text{ ms}$ ,  $T_{e,f} \leq 10 \text{ eV}$ ).

Calculating the generated RE current during the artificial disruption with ASTRA, expected behaviour is obtained, as a thermal quench on shorter time scales down to lower temperatures enhances RE generation (see Fig. 2a)). For the smallest combinations of  $\tau$  and  $T_{e,f}$ , full current conversion is approached. Comparison of the RE currents obtained with calculations by GO

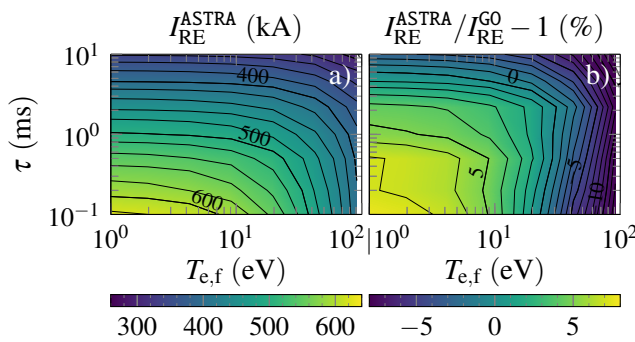


**Fig. 2:** a) Generated RE current calculated by ASTRA in an artificial AUG disruption and b) compared to calculations by GO.

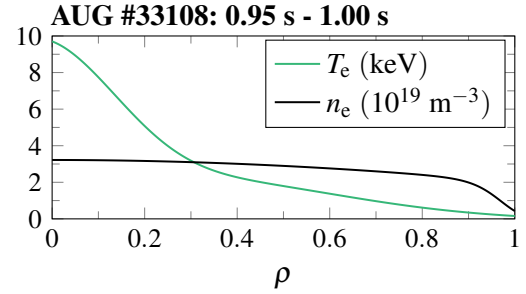


**Fig. 1:** Electron density and temperature of AUG #33108, averaged prior to MGI [3].

shows reasonable agreement in the order of 5% in the experimentally relevant regime (see Fig. 2b)). Given small differences between both tools (e.g. geometric factors, electric field evolution, numerical treatment), the implementation of the fluid equations for RE generation in ASTRA can be considered accurate, thus allowing studies of the interplay between MMI and REs.

#### 4. MMI: Homogeneous Ar deposition

The simplest MMI model assumes homogeneous, instantaneous deposition. Albeit experimentally unrealistic, this case constitutes a sanity check for the toolkit presented. To simulate this deposition scheme, Ar densities in the range  $1 - 10 \times 10^{19} \text{ m}^{-3}$  are prescribed to AUG #33108 at the start of the simulation, corresponding to a total number of injected –

and assimilated – Ar in the range  $0.1 - 1.1 \times 10^{21}$ . Although in AUG #33108  $1.7 \times 10^{21}$  Ar atoms were injected into the vessel, low assimilation yields an expected Ar density of  $(3.7 \pm 1.4) \times 10^{19} \text{ m}^{-3}$  (derived from [1]). Hence in the simulations, Ar densities chosen cover experimental estimates. For simplicity, particle transport is omitted and  $T_i$  set to  $T_e$ . To hinder the emergence of soliton solutions for  $T_e$ , the heat transport coefficient is set to  $\chi_e = 10 \text{ m}^2/\text{s}$ .

The RE current response to a variation of  $n_{\text{Ar}}$  is shown in Fig. 3a). Only a few kA of RE current  $I_{\text{RE}}$  are produced, in contrast to experimental observations of 222 kA. The avalanche mechanism is of minor importance. Despite applying a large value for  $\chi_e$ , emergence of metastable  $T_e$  filaments is encountered (off-axis for  $n_{\text{Ar}} \leq 6.0 \times 10^{19} \text{ m}^{-3}$ ). In these regions with  $T_e \sim 100 \text{ eV}$  and  $\langle Z_{\text{imp}} \rangle \sim 8$ , RE generation is calculated to occur predominantly. In general, depositing more Ar into the plasma increases  $I_{\text{RE}}$ , as a faster thermal quench induces stronger parallel electric fields. However above  $n_{\text{Ar}} = 10 \times 10^{19} \text{ m}^{-3}$ , post-quench  $T_e$  is too low for significant primary RE generation to occur. Since instantaneous deposition is far from realistic, the density profile for  $n_{\text{Ar}} = 1 \times 10^{19} \text{ m}^{-3}$  is ramped up linearly over a duration  $t_{\text{inj}} \leq 5 \text{ ms}$  ( $t_{\text{inj}}^{\text{exp}} = (1.2 \pm 0.1) \text{ ms}$ ) in subsequent simulations (see Fig. 3b)). As a result, the RE current is increased by up to two orders of magnitude for  $1.5 \text{ ms} \leq t_{\text{inj}} \leq 3.0 \text{ ms}$ , reaching values of up to 66 kA. Yet, emergence of  $T_e$ -filaments is observed also in these cases, demanding ad hoc application of reduced turbulent transport models. Consequently, these simple deposition models are not suitable for simulations of Ar MMI in AUG.

#### 5. MGI: Edge Ar injection

Experimental conditions of AUG #33108 are approached by simulating Ar MGI from the outside of the plasma volume for varying injection amounts  $N_{\text{Ar}}$ . Neutrals introduced are assumed to propagate inwards with thermal velocity of  $v_{\text{th}} = 390 \text{ m/s}$  and ions to diffuse with  $D = 1 \text{ m}^2/\text{s}$ . In the simulations performed, the cold neutral gas front propagates effectively with  $v \ll v_{\text{th}}$  due to ionisation of implanted neutrals. Consequently, the penetration velocity is increased when more material is injected. As the gas front reaches the

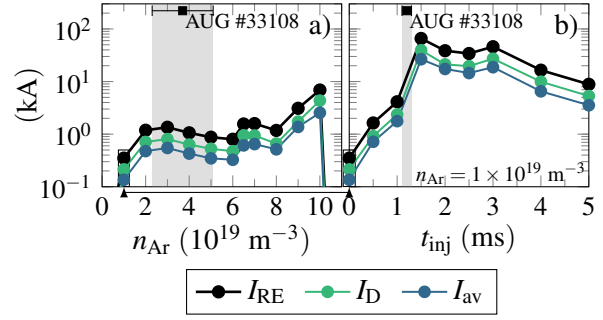


**Fig. 3:** RE current generated for homogeneous Ar MMI, deposited a) instantaneously and b) linearly over a duration  $t_{\text{inj}}$  for  $n_{\text{Ar}} = 1 \times 10^{19} \text{ m}^{-3}$ .

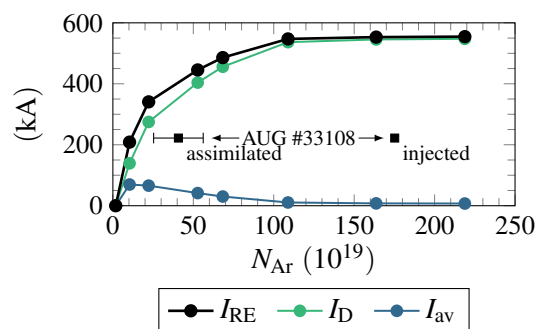


**Fig. 4:** RE current generated for Ar MGI with different injection quantities  $N_{Ar}$  compared to experimental estimates.

Additionally, the Ar assimilation fraction deviates increasingly from unity. It should be noted, however, that several disruption quantities (e.g. temporal evolution, duration, temporal evolution) are still in qualitative disagreement with measurements. Thus, aforementioned simulations are to be repeated in future studies with more accurate plasma parameters, utilization of transport models and consideration of loss mechanisms for the seed REs.

**6. Conclusion** In this work, the toolset ASTRA-STRAHL is presented for the study of Ar MMI in AUG discharges. Simple models for material deposition are found unsuitable to describe RE generation even qualitatively in exploratory simulations. Only with edge injection (MGI), experimental RE behaviour is reproduced qualitatively. For Ar quantities noticeably above experimental levels, full current conversion is approached. Future work will aim at improving experimental agreement through application of optimized models and parameters. Eventually, material delivery through shattered pellet injection [12] is to be investigated.

**Acknowledgements** This work has been carried out within the framework of the EUROfusion Consortium and has received funding from the Euratom research and training program 2014-2018 and 2019-2020 under grant agreement No 633053. The views and opinions expressed herein do not necessarily reflect those of the European Commission.

## References

- [1] G. Pautasso et al., 45<sup>th</sup> EPS Conference on Plasma Physics, 02.-06.07.2018, Prague, Czech Republic, P4.1058
- [2] G. Pautasso et al., *Plasma Phys. Control. Fusion* **59**, 014046 (2017)
- [3] G. Papp et al., This conference, I4.105
- [4] E. Fable et al., *Plasma Phys. Control. Fusion* **55**, 124028 (2013)
- [5] R. Dux et al., *Nucl. Fusion* **39**, 1509 (1999)
- [6] E. Fable et al., *Nucl. Fusion* **56**, 026012 (2016)
- [7] J.W. Connor et al., *Nucl. Fusion* **15**, 415 (1975)
- [8] M.N. Rosenbluth et al., *Nucl. Fusion* **37**, 1355 (1997)
- [9] L. Hesslow et al., *Plasma Phys. Control. Fusion* **60**, 074010 (2018)
- [10] L. Hesslow et al., *Nucl. Fusion* **59**, 084004 (2019)
- [11] G. Papp et al., *Nucl. Fusion* **53**, 123017 (2013)
- [12] G. Pautasso et al., This conference, P4.1045

magnetic axis, the TQ-phase is completed. As opposed to the previous cases,  $T_e$  filaments do not emerge. Even though simulation are performed to demonstrate the toolkit's capabilities, rather than to capture experimental behaviour, the RE current calculated is in the correct order of magnitude for  $N_{Ar} \leq 5 \times 10^{20}$  (see Fig. 4). For noticeably larger values  $N_{Ar} > 10^{21}$ , full current conversion is approached. Again, secondary RE generation is of minor importance.